

Exposure of Rats to Environmental Tobacco Smoke during Cerebellar Development Alters Behavior and Perturbs Mitochondrial Energetics

Brian F. Fuller,^{1,2} Diego F. Cortes,¹ Miranda K. Landis,¹ Hiyab Yohannes,¹ Hailey E. Griffin,¹ Jillian E. Stafflinger,¹ M. Scott Bowers,³ Mark H. Lewis,⁴ Michael A. Fox,¹ and Andrew K. Ottens^{1,2}

¹Department of Anatomy and Neurobiology, and ²Department of Biochemistry and Molecular Biology, Virginia Commonwealth University, Richmond, Virginia, USA; ³Department of Psychiatry, Virginia Institute of Psychiatric and Behavioral Genetics, Virginia Commonwealth University, Richmond, Virginia, USA; ⁴Department of Psychiatry, McKnight Brain Institute of the University of Florida, Gainesville, Florida, USA

BACKGROUND: Environmental tobacco smoke (ETS) exposure is linked to developmental deficits and disorders with known cerebellar involvement. However, direct biological effects and underlying neurochemical mechanisms remain unclear.

OBJECTIVES: We sought to identify and evaluate underlying neurochemical change in the rat cerebellum with ETS exposure during critical period development.

METHODS: We exposed rats to daily ETS (300, 100, and 0 $\mu\text{g}/\text{m}^3$ total suspended particulate) from postnatal day 8 (PD8) to PD23 and then assayed the response at the behavioral, neuroproteomic, and cellular levels.

RESULTS: Postnatal ETS exposure induced heightened locomotor response in a novel environment on par initially with amphetamine stimulation. The cerebellar mitochondrial subproteome was significantly perturbed in the ETS-exposed rats. Findings revealed a dose-dependent up-regulation of aerobic processes through the modification and increased translocation of Hk1 to the mitochondrion with corresponding heightened ATP synthase expression. ETS exposure also induced a dose-dependent increase in total Dnm1l mitochondrial fission factor; although more active membrane-bound Dnm1l was found at the lower dose. Dnm1l activation was associated with greater mitochondrial staining, particularly in the molecular layer, which was independent of stress-induced Bcl-2 family dynamics. Further, electron microscopy associated Dnm1l-mediated mitochondrial fission with increased biogenesis, rather than fragmentation.

CONCLUSIONS: The critical postnatal period of cerebellar development is vulnerable to the effects of ETS exposure, resulting in altered behavior. The biological effect of ETS is underlain in part by a Dnm1l-mediated mitochondrial energetic response at a time of normally tight control. These findings represent a novel mechanism by which environmental exposure can impact neurodevelopment and function.

KEY WORDS: attention deficit/hyperactivity disorder, carbohydrate metabolism, cerebellum, environmental tobacco smoke, mitochondrial biogenesis, mitochondrial energetics, neurodevelopment, proteomics, secondhand smoke, systems biology. *Environ Health Perspect* 120:1684–1691 (2012). <http://dx.doi.org/10.1289/ehp.1104857> [Online 26 September 2012]

Recent epidemiological studies find a dose-dependent increased risk for behavioral and cognitive problems and a greater incidence of mental disorders in children exposed to environmental tobacco smoke (ETS) (Anderko et al. 2010; Bandiera et al. 2011; Kabir et al. 2011). Confirming earlier findings, these studies addressed two major concerns highlighted in the U.S. Surgeon General report on ETS health consequences by employing objective biomarker measurements and determining that effects are independent of maternal smoking (U.S. Department of Health and Human Services 2006). Thus, nearly one in five U.S. children are at greater risk for mental health problems because of postnatal ETS exposure, a prevalence that has remained unchanged for over a decade (Centers for Disease Control and Prevention 2010). ETS exposure is more pronounced in the young because of their higher respiration rates and remains prevalent because 50% of mothers who cease smoking during pregnancy resume < 6 months after delivery (Colman

and Joyce 2003; Marano et al. 2009). The issue is of even greater concern worldwide, with over 50% of children regularly exposed to ETS across large parts of Europe and Asia (Oberg et al. 2011). Yet, it remains undetermined whether early ETS exposure directly affects neurodevelopment to induce behavioral change and what biological mechanisms might underlie its effects.

Activity, attention, impulsivity, and language deficits, which have been reported with greater incidence in ETS-exposed children, all involve cerebellar regulation through feedback loops to the neocortex (Bledsoe et al. 2011; O'Halloran et al. 2012; Richter et al. 2005). Reduced cerebellar size and function have also been associated with attention deficit hyperactivity disorder (ADHD) and conduct disorders (Aguiar et al. 2010; Dalwani et al. 2011; O'Halloran et al. 2012; Richter et al. 2005). A meta-analysis of ADHD structural imaging studies found reproducible cerebellar abnormalities in areas of the posterior cerebellum, such as in lobule VIII (Valera et al.

2007). These results suggest cerebellar vulnerability that may be linked with its late development in mammals, including humans. Research by Dobbing and colleagues established the precept of a vulnerable period for neurodevelopment as reviewed elsewhere (Dobbing 1982), which in the human cerebellar cortex extends > 1 year after birth, rendering it susceptible to the effects of postnatal ETS (Dobbing 1982; Friede 1973; Koop et al. 1986). Corresponding rat cerebellar cortex development extends approximately between postnatal day (PD) 8 and PD24 (Altman and Bayer 1997; Gramsbergen 1993) and has been shown to be vulnerable to various insults, with lasting morphological and functional deficits (Altman and Bayer 1997; Bedi et al. 1980; Dobbing 1982). In the present study, we exposed rat pups to daily ETS [300, 100, and 0 $\mu\text{g}/\text{m}^3$ total suspended particulate (TSP)] during the cerebellar vulnerable period, a rational initial point of investigation given its postnatal vulnerability and functional relevance to reported deficits and disorders. More broadly, this study *a)* addresses a lack of knowledge of the neurobiological effects of ETS during development, and *b)* studies potential mechanistic underpinnings.

Address correspondence to A.K. Ottens, Department of Anatomy and Neurobiology, Virginia Commonwealth University, PO Box 980709, Richmond, VA 23298-0709 USA. Telephone: (804) 628-2972. Fax: (804) 828-9477. E-mail: akottens@vcu.edu

Supplemental Material is available online (<http://dx.doi.org/10.1289/ehp.1104857>).

We are grateful for assistance from Y. Tanimura and B. McLaurin with animal handling; R. Hamm for behavioral testing; A. Lichtman and S. O'Neal for the use of the ANY-Maze system; S. Geromanos, H. Vissers, and M. Gorenstein for informatics; and J. Williamson, S. Henderson, P. Trimmer, L. Phillips, T. Reeves, and T. Smith for electron microscopy, performed at the VCU Department of Anatomy and Neurobiology Microscopy Facility, which is supported with funding from National Institutes of Health, National Institute of Neurological Disorders and Stroke (NIH-NINDS) grant NS047463.

This research was supported in part by NIH-NINDS grant NS055012, NIH National Center for Advancing Translational Sciences, Clinical and Translational Science Award program grant TR000058, and the AD Williams' Fund.

The authors declare they have no actual or potential competing financial interests.

Received 14 December 2011; accepted 26 September 2012.

Materials and Methods

Animal procedures and tissue collection.

Animals were treated humanely and with regard for alleviation of suffering. All procedures conformed to the U.S. Public Health Service policy with local institutional animal care and use committee approval. Pregnant Sprague-Dawley rats were purchased from Harlan Laboratories (Indianapolis, IN) and housed in a facility approved by the Association for Assessment and Accreditation of Laboratory Animal Care on a 12-hr light cycle with *ad libitum* access to food and water. We treated male rat pups daily from age PD8 to PD23 in a Teague TE-10 smoking system (Teague Enterprises, Woodland, CA) operated as described previously (Fuller et al. 2010; Gospe et al. 1996; Slotkin et al. 2001), with TSP levels confirmed daily. The first of two exposure groups received amplified ETS at a mean daily level of 300 $\mu\text{g}/\text{m}^3$ TSP (ETS₃₀₀), with peak concentrations of 2 mg/m^3 during active smoking. The extreme concentration modeled here, which is realistic to ETS in cars (Ott et al. 2008), was used to more readily detect a biochemical response in our initial mechanistic studies. Exaggerated chronic exposure may also be considered relevant for ETS exposure in combination with urban pollution, where mean daily TSP levels can measure in large metropolitan areas in the hundreds of micrograms per cubic meter, principally from other combustion sources (Calderón-Garcidueñas et al. 2008). In a second exposure, we modeled upper quartile ETS levels found in homes with smokers, with a mean daily level of 100 $\mu\text{g}/\text{m}^3$ TSP (ETS₁₀₀) peaking at 0.5 mg/m^3 during active smoking (U.S. Environmental Protection Agency 1992). This exposure approximated ETS levels recorded in bedrooms of preschool children in homes with a pack-a-day smoker (McCormack et al. 2008). Litters cumulatively received 3 hr/day of ETS exposure, apart from dams, with feedings in between. Control animals were handled identically except for not receiving ETS exposure. Mean daily carbon monoxide levels remained < 5 ppm. Animal weight was monitored daily and no difference was found between groups. Brains were collected after the close of the initial cerebellar vulnerability period at PD25.

Locomotor activity. Using previously described procedures (Stohr et al. 1998) with the following modifications, we measured spontaneous locomotor activity in an unfamiliar environment at PD25 during the light cycle (1100–1400 hours). Animals were placed in a 42 × 42 × 30 cm^3 open field arena under red light illumination (1 lux at height of animal). Chambers were located within a sound-isolated room. ETS₁₀₀-exposed animals and one control (Cnt) group received acute saline [Sal; 1 mL/kg, intraperitoneally (ip)] while a second, hyperlocomotor-positive control group

received acute amphetamine (Amp; 1 mg/kg, ip): ETS/Sal, Cnt/Sal, Cnt/Amp. We placed animals in the center of the arena 15 min after injection and recorded activity (total distance traveled, maximum velocity, and entries into a 14 × 14 cm^2 central zone) assessed in 1-min intervals using ANY-maze tracking software (version 4.84; Stoelting, Wood Dale, IL). We cleaned the arena with 90% ethanol with the odor blown off before subsequent testing. The 1-mg/kg amphetamine dose was based on our pilot data indicating the dose would increase locomotor activity without stereotypic behavior. In contrast, both increased locomotion and stereotypic behavior were observed at a 3-mg/kg dose level (data not shown).

Two-dimensional chromatography-tandem mass spectrometry. Tissue from the cerebellar hemisphere was processed through a multi-step protein extraction procedure described previously (Cortes et al. 2012). Briefly, we sequentially homogenized tissue in aqueous and membrane dissociation buffers (matrix and membrane extracts, respectively) to resolve the neuroproteome into matrix-associated and membrane-associated compartments (Cortes et al. 2012). We assayed protein concentration with a Pierce 660 kit (Thermo Scientific, Rockford, IL). Protein samples (50 μg) were reduced, alkylated, trypsin-digested, and concentrated into 20 μL of 100-mM ammonium formate (pH 10). We injected protein digests (4 μL each) in a treatment-interspersed order onto a two-dimensional nanoACQUITY ultra performance liquid chromatography system using an On-Line RP/RP 2D Separations kit ahead of a Synapt HDMS mass spectrometer operated in a data-independent acquisition mode (all from Waters, Milford, MA). We used Waters PLGS software (version 2.4) to process and annotate mass spectral data [using the Uniprot KB Rattus database (<http://www.uniprot.org/taxonomy/10116>)]. We filtered peptide annotations to a 1% false positive identification rate. For label-free quantification, we tabulated all unique peptides from matrix and membrane extracts with their chromatographic peak area intensities across all biological replicates ($n = 8$). Data were \log_2 transformed, normalized, and imputed for nonrandom missing values [for more detail, see Supplemental Material, p. 5 (<http://dx.doi.org/10.1289/ehp.1104857>)].

Interaction informatics. Peptide measures found to be statistically responsive to ETS exposure reflected putative modulation of a parent protein or protein family's abundance, modification, or localization. We performed protein enrichment analysis against Gene Ontology (GO) Annotation terms (biochemical process and cellular component) (GO Consortium, <http://www.geneontology.org/>) and biochemical pathways using a Fisher's inverse chi-square method with Bonferroni

correction [ToppGene (<http://toppgene.cchmc.org/>); initial $\alpha = 0.05$] (Chen et al. 2009). Further detail on enriched pathways was assessed through the KEGG Pathway Database (Kanehisa et al. 2010). Proteins associated with the GO term mitochondrion GO:0005739, the most significant enriched cellular component, were analyzed further using protein-protein network analysis [STRING version 8.3 (Szklarczyk et al. 2011)] with the following parameters: a minimum interaction confidence score of 0.5, ≤ 10 interactors, and displayed in evidence view applying a Markov Cluster algorithm.

Immunoblot analysis. We resolved protein-balanced samples (10 μg) using the NuPAGE gel system with 4–12% Bis-Tris gels, and MOPS running buffer (Life Technologies, Grand Island, NY). The samples were then transferred to a polyvinylidene fluoride membrane (Millipore, Billerica, MA) via a semi-dry method using NuPAGE transfer buffer (Life Technologies). We then probed the membrane with anti-mouse hexokinase-1 (Hk1) (Sigma-Aldrich, St. Louis, MO), anti-mouse ATP synthase 5A (ATP5A) (Abcam, Cambridge, MA), or anti-rabbit dynamin-1-like (Dnm1l) protein (Origene, Rockville, MD). We used IgG horseradish peroxidase-conjugated secondary antibodies and the SuperSignal West Pico chemiluminescence detection kit (Thermo Scientific) for imaging. Blots were re-probed with anti-mouse β -actin (Abcam) to control for load error. We acquired 16-bit blot images on an Image Station 4000MM Pro imager (Carestream Health, Rochester, NY) and measured net band intensity.

Immunofluorescence microscopy. Cerebellar hemisphere tissues were sagittally cryosectioned (10 μm) from 2–2.25 mm lateral of midline and fixed with 3% paraformaldehyde. Sections were probed with anti-mouse mitofilin (MitoSciences, Eugene, OR), anti-rabbit Dnm1l (Origene), and anti-rabbit Calbindin1 (Swant, Marly, Switzerland). We used Alexa Fluor conjugated secondary antibodies (Life Technologies) to acquire at least four images per lamina in lobule VIII from four sections on a Zeiss AxioImager A1 fluorescence microscope (Carl Zeiss, Oberkochen, Germany) using identical parameters. Images were analyzed blind to treatment with relative fluorescent intensity measured for regions of interest using ImageJ software (Abramoff et al. 2004).

Transmission electron microscopy. Additional sagittal sections from ETS and control tissues described above were collected at a 50- μm thickness. They were fixed with 2% glutaraldehyde/2% paraformaldehyde (60 min at 4°C), and post-fixed in 1% osmium tetroxide (2 hr). Afterward, sections were dehydrated through a graded ethanol series (50–100%), transitioned through propylene oxide, and then infiltrated overnight

in Embed 812 (Electron Microscopy Sciences, Hatfield, PA). We collected thin sections (80 nm) by ultramicrotomy onto copper 300-mesh thin bar grids and contrasted the sections in lead citrate and uranyl acetate. We used a Jeol JEM-1230 transmission electron microscope (Tokyo, Japan) to collect digital micrographs. Morphometric stereological analysis of mitochondria was performed about the medial neuropil of the cerebellar molecular layer (Gosker et al. 2007; Siskova et al. 2010). Measurements included the mitochondrial fractional area (FA), the mean mitochondrial profile area (MA), and the mean number of mitochondria per area (MD). Mitochondrial profiles were counted and circled if they fell within a counting frame grid placed sequentially-randomly five times per section as optimized from pilot images in order to measure 100–200 mitochondria per animal (Mouton 2002). We also assessed mitochondrial structure among subpopulations localized within the soman and processes of Purkinje, granular, and glial cells.

Statistical analysis. We evaluated locomotor activity using general linear model multivariate testing and least significant difference post hoc comparisons ($\alpha = 0.05$) in SPSS

(version 20; IBM, Armonk, New York). We used one-way ANOVA (analysis of variance) testing on normalized neuroproteomic data using DanteR software (Audinate, Portland, OR) [see Supplemental Material, p. 5 (<http://dx.doi.org/10.1289/ehp.1104857>)]. We corrected for multiple peptide measures using the Benjamini-Yekutieli false discovery rate method to control type 1 error to 5% (Benjamini and Yekutieli 2001). We loaded normalized immunoblot data in ratio to corresponding β -actin data. Immunoblot and microscop data were tested using either Student's *t*-test or a two-way ANOVA with the Holm-Sidak method ($\alpha = 0.05$).

Results

ETS exposure during postnatal cerebellar development heightens locomotor activity. Our model of ETS exposure resulted in heightened locomotor activity in a novel environment. We found a significant main effect of ETS exposure for measures of distance traveled ($F_{1,28} = 26.49$, $p = 1.9E^{-5}$), maximum velocity ($F_{1,28} = 8.7$, $p = 0.006$) and entries into the center zone of the test arena ($F_{1,28} = 6.5$, $p = 0.017$). Figure 1 displays the time course of habituation to the novel environment and representative

locomotor track plots for each group. Post hoc comparisons across time are illustrated as being significantly different between ETS₁₀₀-exposed animals (ETS/Sal) relative to a matched air-exposed group (Cnt/Sal) as well as to an air-exposed group stimulated with amphetamine (1 mg/kg, Cnt/Amp). We used the Cnt/Amp group as a positive control for a heightened locomotor response, which, as expected, maintained a higher asymptotic level of locomotor activity during and after habituation. When placed in a novel environment, ETS/Sal animals initially exhibited a locomotor phenotype resembling that of Cnt/Amp-stimulated animals. While ETS/Sal animals were more reactive (i.e., exhibited more locomotion) to a novel environment than Cnt/Sal animals, they eventually achieved the same baseline as Cnt/Sal animals during the second half of the session.

ETS induces underlying cerebellar mitochondrial subproteome perturbation and up-regulates aerobic respiration machinery. To begin to understand the neurodevelopmental effects of ETS exposure and the underlying mechanisms of action, we employed a systems-based approach beginning with unbiased proteomic analysis. Bioinformatic assessment [see Supplemental Material, Figure S1 (<http://dx.doi.org/10.1289/ehp.1104857>)] of neuroproteomic change after daily ETS₃₀₀ exposure revealed 662 responsive peptide measures (Figure 2A) that denoted translational and posttranslational dynamics among 389 proteins. This ETS-responsive neuroproteome particularly overrepresented change to the mitochondrial subproteome (103 proteins representing 28% of mitochondrion GO term GO:0005739, $p = 5.33E^{-29}$). All three major aerobic respiration pathways responded to ETS exposure (Figure 2B). This included significant modulation of all glycolytic enzymes, 16 proteins involved in downstream pyruvate processing (e.g., 5 of 8 tricarboxylic acid cycle enzymes), and 10 subunits of four electron transport chain complexes [see Supplemental Material, Figure S2 (<http://dx.doi.org/10.1289/ehp.1104857>)]. These data revealed that ETS exposure during cerebellar cortex development prominently influenced mitochondria and, in particular, processes involved in aerobic function.

We next assessed the regulational state of aerobic metabolism, which is governed by posttranslational dynamics of the rate-limiting enzyme Hk1. Hk1 peptide measures (Figure 2C) indicated a treatment-induced shift in localization. Mass spectrometry also revealed three previously unknown phosphorylated and glycosylated Hk1 motifs that were responsive to ETS₃₀₀ exposure (Hk1-modified peptides) [Figure 2C; see also Supplemental Material, Figure S3 (<http://dx.doi.org/10.1289/ehp.1104857>)]. We further affirmed that Hk1

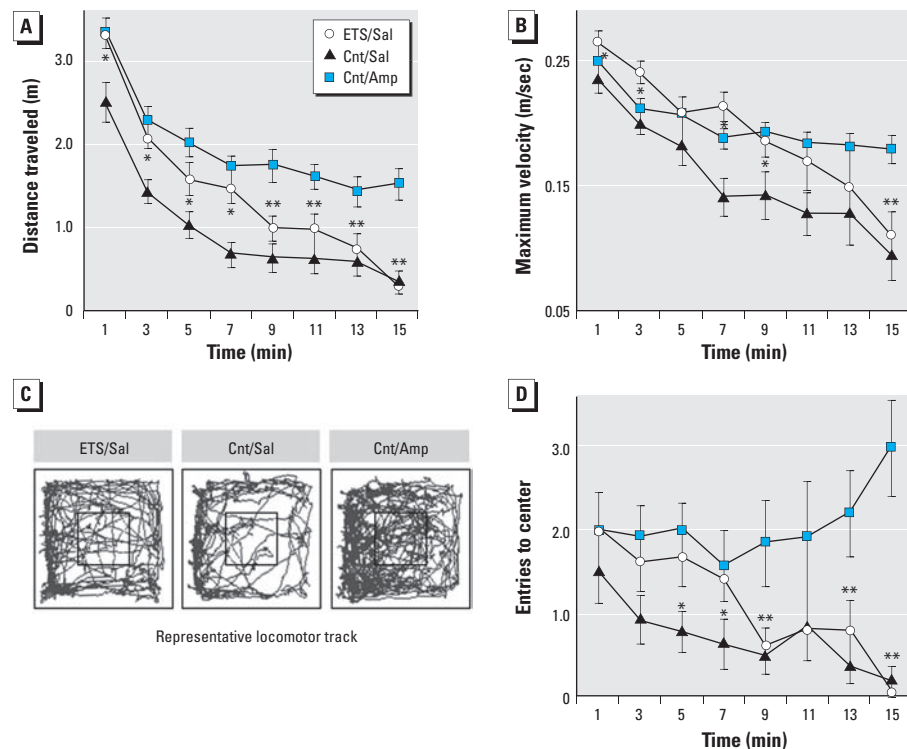


Figure 1. Spontaneous locomotor activity is increased after postnatal ETS exposure. After initial rat cerebellar cortex formation, locomotor activity in a $42 \times 42 \times 30$ cm³ open field was recorded at PD25 for ETS₁₀₀-exposed or plain-air control (Cnt) animals. Amphetamine (Amp; 1 mg/kg) as a hyperlocomotion positive control or saline vehicle (Sal) was injected ip 15 min previously. (A) Plot of total distance traveled quantified in 1-min bins. (B) Plot of maximum velocity quantified in 1-min bins. (C) Locomotor track plots for those animals with a median measure of total distance traveled per treatment group; 14×14 cm² central zone shown boxed. (D) Plot of entries into the central zone quantified in 1-min bins. Data are presented as mean \pm SE; $n = 14$ /group.

* $p < 0.05$ ETS/Sal compared with Cnt/Sal; ** $p < 0.05$ ETS/Sal compared with Cnt/Amp.

translocation was dose-dependent with 45% and 22% shifts to the mitochondrial membrane relative to controls after ETS₃₀₀ and ETS₁₀₀ exposures, respectively (Figure 2D). We also observed an ETS₃₀₀-induced increase in peptide levels of ATP synthase (ATP5) (Figure 2E), which exhibited a dose-dependent 51% or 23% response to ETS₃₀₀ and ETS₁₀₀ exposures, respectively, over matched controls (Figure 2F).

ETS stimulates Dnm11 mitochondrial fission independent of stress-induced Bcl2 family dynamics. We examined whether the significant up-regulation of aerobic respiration machinery co-occurred with altered mitochondrial fission/fusion dynamics. The ETS-responsive neuroproteome revealed significant modulation of the mitochondrial fission factor Dnm11 (or Drp1), whereas the mitochondrial fusion factor mitofusin was

unresponsive to ETS exposure. Dnm11 peptide measures reflected a significant increase with ETS₃₀₀ exposure (Figure 3A). We further measured 35% less phosphorylation at S₆₁₅ (S₅₉₆ in human) relative to control ($p = 0.026$) by tandem mass spectrometry (Figure 3B). After ETS₃₀₀ exposure, we measured a robust 125% increase in cytosolic Dnm11; however, a lower 53% increase in mitochondria-bound Dnm11 did not reach significance at $p = 0.15$

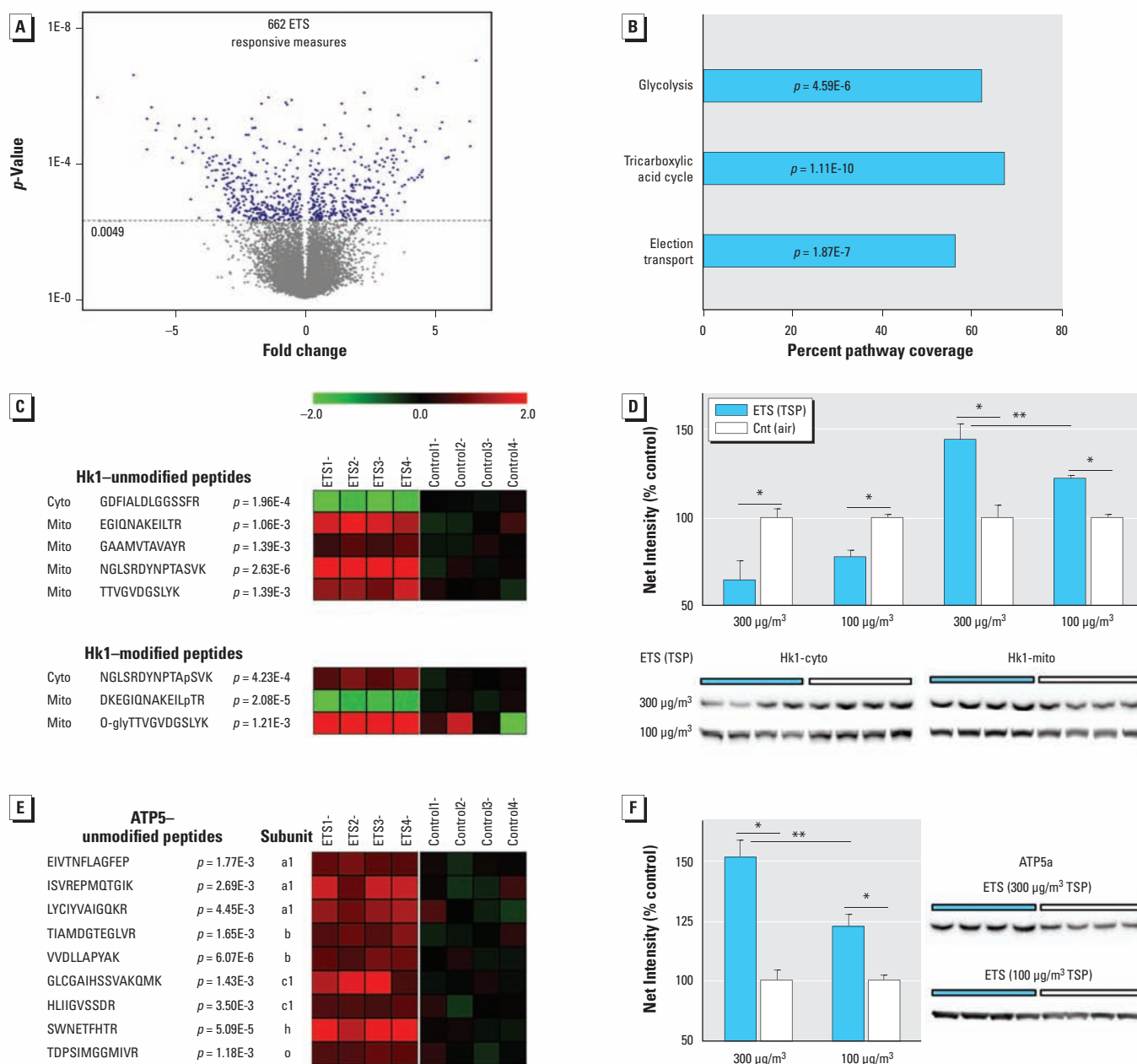


Figure 2. Significant cerebellar proteome perturbation after ETS exposure with dose-dependent up-regulation of aerobic processes. Animals were exposed daily to ETS or plain air (Cnt). (A) Quantitative proteomics revealed 662 ETS₃₀₀-exposure responsive peptides in the cerebellar cortex, denoting significant change among 389 proteins; data are presented as fold change ($n = 4/\text{group}$; corrected $\alpha = 0.0049$). (B) Aerobic respiration pathways prominently altered in the ETS-responsive neuroproteome; data are presented as percent pathway coverage (corrected $\alpha = 0.016$). (C,E) Heatmap plots of ETS₃₀₀-responsive peptide measures for Hk1 (C; unmodified and posttranslationally modified) and ATP5 (E) (log₂ ratio to control; $n = 4/\text{group}$; p -values reported). (D,F) Dose-dependent immunoblot protein measures of Hk1 (D) and ATP5a (F); cytosolic (cyto) and mitochondrial (mito) protein levels graphed for Hk1 to assess subcellular translocation. Data are presented as mean \pm SE; $n = 4/\text{group}$.

* $p < 0.05$ compared with controls. ** $p < 0.01$ compared across dose.

(Figure 3C). In sharp contrast, the milder ETS₁₀₀ exposure induced a 311% increase in active membrane-bound Dnm1I over controls, while the 32% increase in cytosolic Dnm1I was more in line with a dose-dependent effect of exposure. Increased Dnm1I staining was more broadly distributed across molecular (ML) and Purkinje (PL) laminae of ETS₁₀₀-exposed animals relative to controls (Figure 3D and D', respectively). We further observed a corresponding increase in mitochondrial marker staining (MF), with Dnm1I-stained puncta found adjacent to MF-stained mitochondria. We assayed the Bcl-2 family

members Bcl-X_L and BBC3, which are known modulators of mitochondrial dynamics and Dnm1I; however, both were found unchanged with ETS exposure (Figure 3E).

ETS induces mitochondrial biogenesis, not fragmentation, in cerebellar cortex. We further evaluated the extent and nature of Dnm1I-mediated mitochondrial fission. As previously shown with ETS₁₀₀ exposure, ETS₃₀₀ exposure significantly increased mitoflin-stained mitochondria within the ML and PL (Figure 4A). In contrast, granular layer (GL) mitochondrial staining was also heightened with ETS₃₀₀ exposure. Mean immunofluorescence intensity

was significantly greater in all three laminae (Figure 4B), with the greatest increase relative to control in the ML. To explore whether these results were consequent to an increase in mitochondrial fragmentation (degeneration), network size, or biogenesis we examined mitochondrial morphology by electron microscopy. Morphometric stereological analysis affirmed that the fractional area occupied by mitochondria in the ML doubled with ETS₃₀₀ exposure relative to controls (Figures 4D,D'), which closely agreed with our immunofluorescence data. The mean profile area, an indication of mitochondrial size, showed no

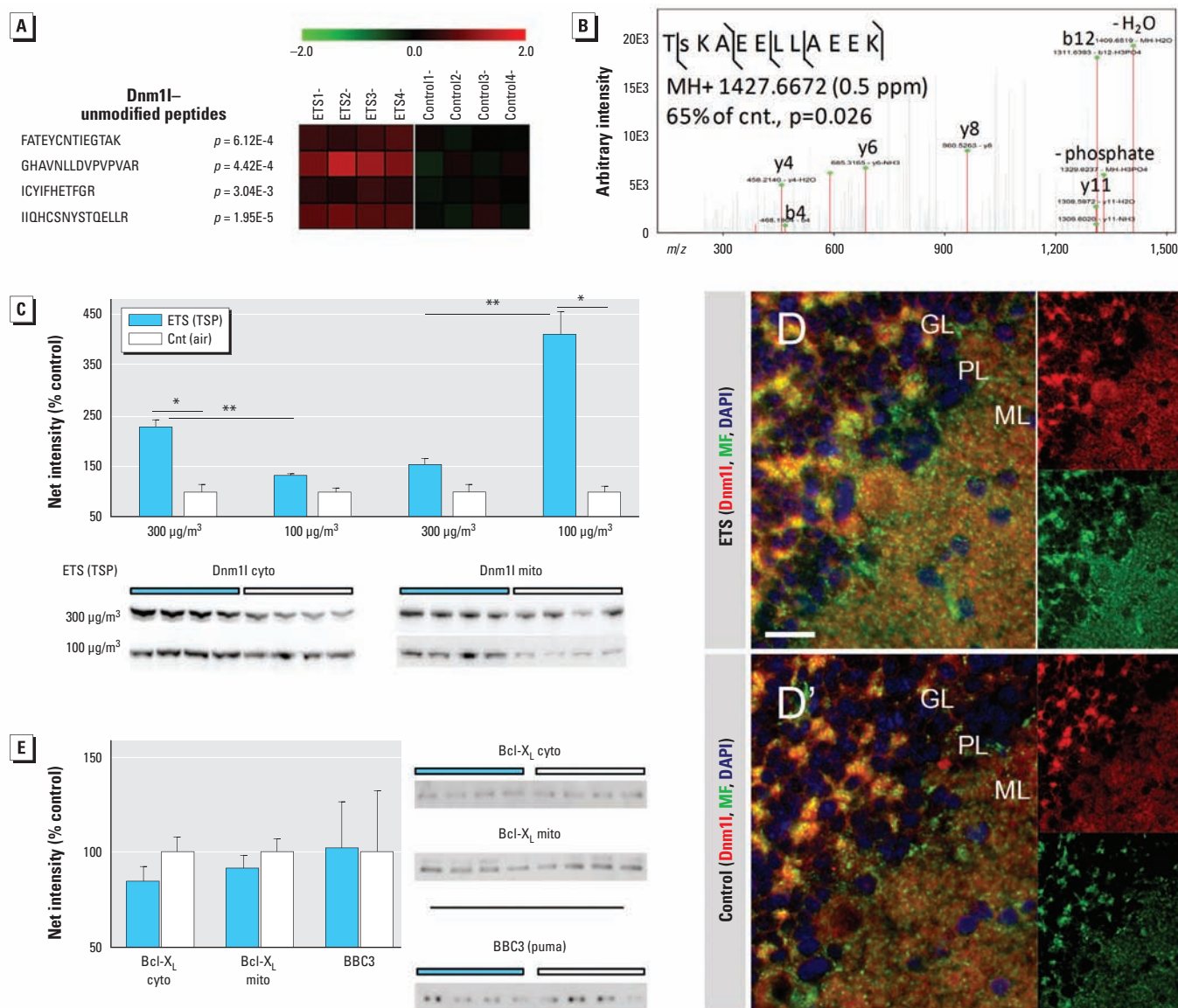


Figure 3. ETS stimulates Dnm1I-mediated mitochondrial fission independent of stress-induced Bcl-2 family dynamics. Animals were exposed daily to two levels of ETS (300 $\mu\text{g}/\text{m}^3$ or 100 $\mu\text{g}/\text{m}^3$ TSP) or plain air (Cnt). (A) Heatmap of fission factor Dnm1I unmodified peptide measures within the ETS-responsive neuroproteome. (B) Tandem mass spectrum confirming reduced phosphorylation at S₆₁₅ (Log₂ ratio to control; $n = 4/\text{group}$). (C) Protein levels of cytosolic (cyto) and mitochondrial (mito) Dnm1I were measured by immunoblot. (D,D') Color-coded coimmunofluorescence staining of Dnm1I, the mitochondrial marker mitoflin (MF), and 4',6-diamidino-2-phenylindole (DAPI) in cerebellar cortex of ETS₁₀₀-exposed (D) and air-control animals (D'); granular (GL), Purkinje (PL), and molecular (ML) laminae are demarked, and Dnm1I and MF channels are displayed separately on right; bar = 20 μm . (E) Protein levels of Bcl-2 family members were measured by immunoblot analysis, indicating no significant response to ETS exposure. Data are presented as mean \pm SE; $n = 4/\text{group}$.

* $p < 0.001$ compared with controls. ** $p < 0.001$ compared across dose.

statistical difference between groups, whereas the count of mitochondrial profiles per field was significantly greater at double that of control. Qualitative assessment of micrographs localized the greater mitochondrial density particularly to Purkinje dendrites in the ML of ETS-exposed animals relative to controls (Figures 4C,C'). Yet, mitochondrial ultrastructure remained consistent and healthy appearing between groups (Figure 4E,E'), with no distinguishable morphological difference from control to suggest stress-induced fragmentation across neuronal and glial subpopulations within the GL, PL, and ML [see Supplemental Material, Figure S4 (<http://dx.doi.org/10.1289/ehp.1104857>)].

Discussion

To our knowledge, these are the first findings to demonstrate a significant effect of postnatal ETS exposure on behavior and a potential underlying mechanism involving perturbed mitochondrial energetics critical

to the developing brain. This novel insight into the pathobiological impact of ETS during a vulnerable period is the product of a systems-based approach using unbiased proteomic assessment. Prenatal maternal exposure to cigarette smoke has been well documented to induce neurological as well as many other lasting health effects as reviewed elsewhere (Doherty et al. 2009; Pauly and Slotkin 2008). Yet, very few studies have explored neurobiological effects relevant to postnatal ETS exposure, despite mounting evidence for adverse behavioral and cognitive outcomes. Thus, we believe results from this study represent a significant advance in the limited knowledge affirming neurobehavioral and neurobiological effect of ETS exposure during development.

Cerebellar perturbation can broadly impact regulation of behavioral and cognitive domains (Steinlin 2008). Our results show that animals exposed to ETS during postnatal cerebellar development exhibited heightened locomotor activity in a novel environment with a slower

rate of habituation relative to controls. The initial heightened locomotor response of the ETS/Sal group was remarkably similar to that of animals injected with a moderate amphetamine dose (Cnt/Amp). These findings were observed across three different dependent measures for the first half of the session. Further, ETS/Sal animals were slower to habituate than either control group, but reached a similar baseline activity to Cnt/Sal animals during the last half of the session. These data suggest an increased response and diminished ability to habituate to an unfamiliar open area rather than a persistent hyperlocomotor response as observed with amphetamine stimulation. Such a behavioral phenotype might result from an ETS-mediated perturbation of inhibitory control loops between cerebellum and neocortex that govern action control (Altman and Bayer 1997). Altman and Bayer (1997) demonstrated that late perturbation during the rat cerebellar vulnerable period, as studied here for ETS, selectively induced (potentially hazardous)

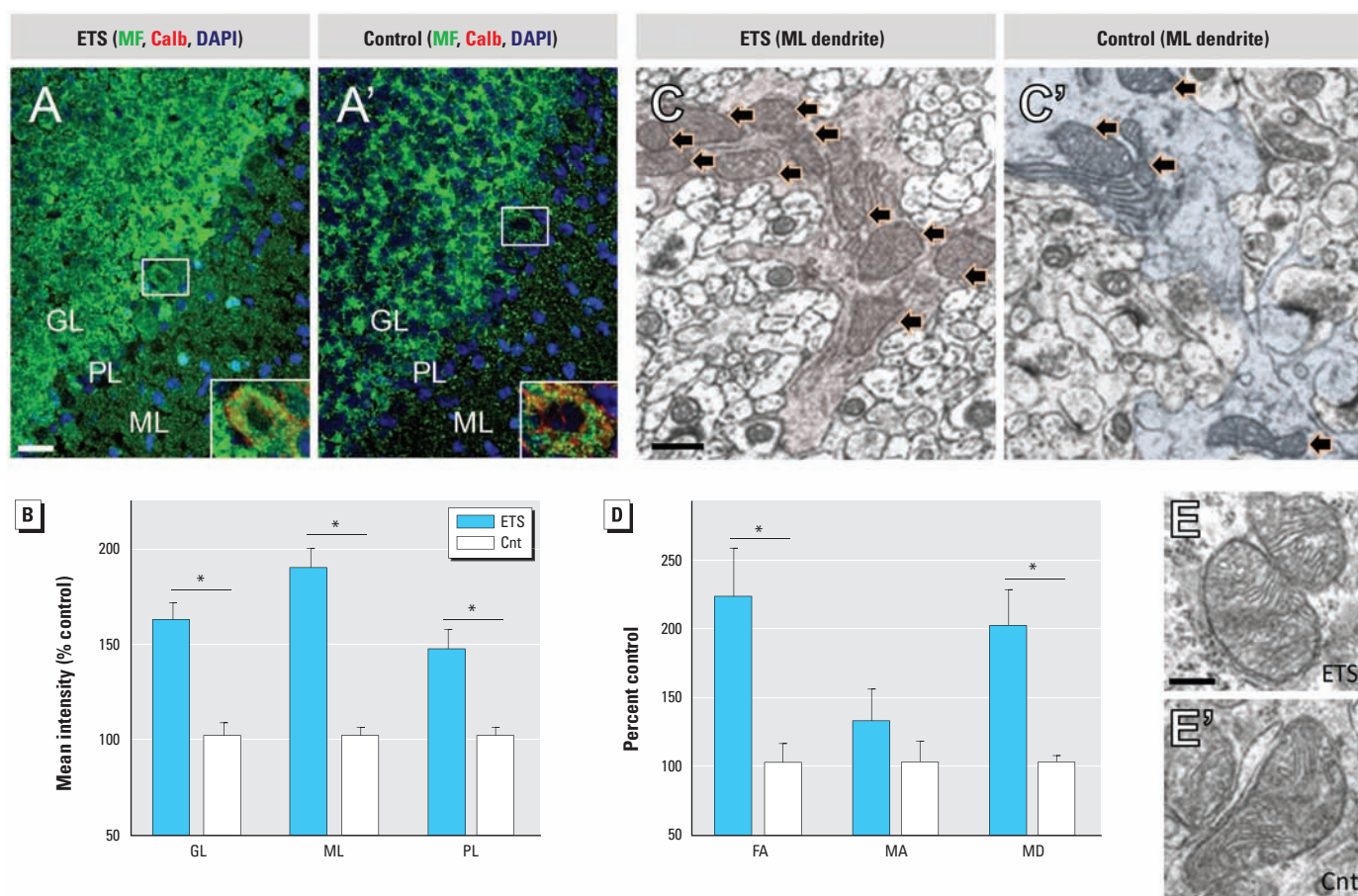


Figure 4. ETS induces Dnm11-mediated mitochondrial biogenesis, not fragmentation, in cerebellar cortex. (A,A') The density of mitochondrial staining (MF) increased in ETS₃₀₀-exposed animals (A) relative to air controls (A') throughout cerebellar cortex; color-coded representative images; bar = 20 μ m; Purkinje cell staining magnified in inset. (B) Mean MF immunofluorescence intensity was significantly greater in granular layer (GL), Purkinje layer (PL), and molecular layer (ML) of cerebellar cortex. (C,C') Representative electron micrographs show more mitochondria within ML Purkinje dendrites (black arrows) of ETS-exposed animals (C) relative to control (C'). (D) Stereological measures of mitochondrial profiles within the ML; mean mitochondrial fractional area (FA), mitochondrial profile area (MA), and mitochondrial density (MD). (E,E') Mitochondrial ultrastructure appears healthy and consistent between ETS-exposed (E) and control (E') animals; representative images from the ML; bar = 200 nm. Data are presented as mean \pm SE; $n = 4$ /group.

* $p < 0.01$ compared with controls.

heightened activity by impacting late ML synaptic development. These findings stand in contrast to the generalized mobility deficits seen with cell loss after early cerebellar insult.

The functional deficits seen in ETS-exposed children suggest perturbation to circuits involving multiple brain regions, and indeed we previously observed change in the frontal cortex, hippocampus, and cerebellum after modeled adult ETS exposure (Fuller et al. 2010). However, the mechanistic studies here warranted anatomical focus. Cerebellar development was a rational point of investigation given extended postnatal vulnerability and relevance to deficits and disorders impacted by ETS exposure in children. Interestingly, Gospe et al. (1996) in the first neurobiological study to model postnatal ETS exposure showed a greater effect in hindbrain over forebrain, suggesting cerebellar susceptibility. Present findings affirm a significant neurobiological effect of postnatal ETS exposure on the cerebellum, including at household-relevant levels. We further identified perturbed mitochondrial energetics as an important underlying mechanism given the correlation to neuronal activity (Kann and Kovacs 2007).

Aerobic demands increase postnatally with heightened synaptic development, requiring more ATP to maintain membrane polarity. Our results show that developmental ETS exposure perturbed mitochondria and associated aerobic pathways. Hk1 is a key regulator of aerobic ATP production, governed by dynamic recruitment from the cytosol to the mitochondrial membrane (de Cerqueira Cesar and Wilson 2002). Our data reveal a dose-dependent shift in Hk1 to the mitochondrial membrane with ETS exposure. Hk1 translocation involves a positive-feedback mechanism with ATP5 utilizing yet unknown posttranslational signaling to alter Hk1 conformation and binding (Hashimoto and Wilson 2000; Pastorino and Hoek 2008). Our results show a corresponding dose-dependent increase in ATP5 and modification of three previously unreported Hk1 posttranslational motifs in response to ETS exposure. Indeed, these modification sites might be found to govern Hk1 dynamics under aerobic respiration with future research.

Brain energetics is further regulated through mitochondrial fission/fusion dynamics. The ETS-responsive neuroproteome reveals significant up-regulation and modification of fission factor Dnm11. Predominantly in the cytosol, Dnm11 initiates fission when recruited to the mitochondrial membrane after posttranslational modification (Baloh 2008; Berman et al. 2008; Uo et al. 2009). Dnm11 was significantly dephosphorylated at S₆₁₅, a motif believed to inhibit function, that is, Dnm11 activity is disinhibited after ETS exposure (Corradino and De Palma

2011; De Palma et al. 2010). Greater Dnm11-stained puncta were found localized with mitochondria, particularly within the ML, with localization to Purkinje dendrites observed by electron microscopy. Heightened ML plasticity critical to cerebellar function remains ongoing through childhood into adolescence (Tiemeier et al. 2010). Interestingly, Li et al. (2008) reported Dnm11 involvement in synaptogenesis as well as mitochondrial biogenesis during development. Our findings may also correlate or perhaps compensate for ETS-altered maladaptive synaptic organization given the close relationship between mitochondrial energetics and synaptogenesis and plasticity in the brain. Thus, the relationship between Dnm11-mediated mitochondrial biogenesis and aberrant synaptic formation or function after ETS exposure warrants future exploration.

Our results also refute the alternative of oxidative stress-induced mitochondrial fragmentation, which too is mediated by Dnm11. Cigarette smoke is well known to induce oxidative stress in other organs resulting in mitochondrial dysfunction and a pro-apoptotic environment involving Bcl-2 family signaling (Armani et al. 2009; Westbrook et al. 2010). In particular, Bcl-X_L binds and activates Dnm11 fission under oxidative-stress conditions (Wu et al. 2011). Yet, our results demonstrate that Bcl-X_L is unresponsive to ETS exposure. Likewise, ETS exposure did not affect levels of pro-apoptotic Bcl-2 binding component 3. Mitochondrial structure appeared undisturbed with ultrastructural analysis. The ETS-responsive neuroproteome lacked a significant association with oxidative stress or apoptotic pathways. Moreover, oxidative stress is known to reduce aerobic respiration, in contrast with our finding of up-regulated aerobic processes. Together, these results support that Dnm11 activation occurs independent of stress-induced Bcl-2 family dynamics and that mitochondrial fragmentation is not occurring in the cerebellum after ETS exposure.

Importantly, we found a dose dependency in the biochemical response to ETS exposure. Most measured changes were halved in response to a 3-fold reduction in ETS levels. These data suggest that a further 3-fold reduction in ETS exposure could still result in a significant effect, assuming a linear relationship, which suggests relevance across a majority of household exposure. Critically, our results show a greater increase in active mitochondrion-tethered Dnm11 after lower ETS₁₀₀ exposure relative to control despite lower overall expression of the protein relative to ETS₃₀₀ exposure. Future studies are needed to demonstrate an effect at lower-level or low-incidence ETS exposure. Also of importance is the interaction between ETS and chronic urban air pollution given prevalent co-exposure. Recently, Calderón-Garcidueñas et al. (2011) showed

that severe (heightened TSP) urban air pollution is also a risk factor for attention, language, and learning cognitive deficits, suggesting potential for a synergistic effect.

Conclusion

In summary, ETS exposure modeled during the postnatal vulnerable period of cerebellar development resulted in a behavioral phenotype and underlying perturbation to mitochondrial energetics in cerebellum that suggest an effect on action control. Our findings further support a biological mechanism involving perturbation to Dnm11-mediated mitochondrial proliferation during critical postnatal cerebellar development, which presents an opportunity for pharmacological intervention. Ongoing cerebellar development, particularly in the molecular layer, is dependent on tight regulation of mitochondrial dynamics. Our data affirm an association of increased Dnm11 activity with mitochondrial biogenesis rather than fragmentation mediated through Bcl-2 family regulation under oxidative stress. Our findings may also have broader implications for other environmental exposures—given that ETS comprises a wide range of toxic chemicals, heavy metals, and combustion particulate matter—and other neuropsychiatric conditions. More recently, cerebellar dysfunction is also being recognized as involved in schizophrenia and autism (O'Halloran et al. 2012). All together, our findings represent a significant contribution to the limited knowledge on the neurodevelopmental effects of ETS exposure and emphasize a mechanism of action involving cerebellar perturbation. By revealing a plausible biological link with mental health disorders, these findings further encourage efforts to eliminate children's exposure to ETS. Our results also support the therapeutic potential targeting of mitochondrial dynamics to treat ETS-induced neurobehavioral and cognitive deficits that affect long-term quality of life.

REFERENCES

- Abramoff MD, Magalhaes PJ, Ram SJ. 2004. Image processing with ImageJ. *Biophotonics Int* 11:36–42.
- Aguiar A, Eubig PA, Schantz SL. 2010. Attention deficit/hyperactivity disorder: a focused overview for children's environmental health researchers. *Environ Health Perspect* 118:1646–1653.
- Altman J, Bayer SA. 1997. Development of the Cerebellar System: In Relation to its Evolution, Structure, and Functions. Boca Raton, FL: CRC Press.
- Anderko L, Braun J, Auinger P. 2010. Contribution of tobacco smoke exposure to learning disabilities. *J Obstet Gynecol Neonatal Nurs* 39:111–117.
- Armani C, Landini L Jr, Leone A. 2009. Molecular and biochemical changes of the cardiovascular system due to smoking exposure. *Curr Pharm Des* 15:1038–1053.
- Baloh RH. 2008. Mitochondrial dynamics and peripheral neuropathy. *Neuroscientist* 14:12–18.
- Bandiera FC, Richardson AK, Lee DJ, He JP, Merikangas KR. 2011. Secondhand smoke exposure and mental health among children and adolescents. *Arch Pediatr Adolesc Med* 165:332–338.
- Bedi KS, Hall R, Davies CA, Dobbing J. 1980. A stereological

- analysis of the cerebellar granule and Purkinje cells of 30-day-old and adult rats undernourished during early postnatal life. *J Comp Neurol* 193:863–870.
- Benjamini Y, Yekutieli D. 2001. The control of the false discovery rate in multiple testing under dependency. *Ann Stat* 29:1165–1188.
- Berman SB, Pineda FJ, Hardwick JM. 2008. Mitochondrial fission and fusion dynamics: the long and short of it. *Cell Death Differ* 15:1147–1152.
- Bledsoe JC, Semrud-Clikeman M, Pliszka SR. 2011. Neuroanatomical and neuropsychological correlates of the cerebellum in children with attention-deficit/hyperactivity disorder—combined type. *J Am Acad Child Adolesc Psychiatry* 50:593–601.
- Calderón-Garcidueñas L, Engle R, Mora-Tiscareño A, Styner M, Gómez-Garza G, Zhu H et al. 2011. Exposure to severe urban air pollution influences cognitive outcomes, brain volume and systemic inflammation in clinically healthy children. *Brain Cogn* 77:345–355.
- Calderón-Garcidueñas L, Solt AC, Henriquez-Roldan C, Torres-Jardon R, Nuse B, Herritt L, et al. 2008. Long-term air pollution exposure is associated with neuroinflammation, an altered innate immune response, disruption of the blood-brain barrier, ultrafine particulate deposition, and accumulation of amyloid β -42 and α -synuclein in children and young adults. *Toxicol Pathol* 36:289–310.
- Centers for Disease Control and Prevention. 2010. Vital signs: non-smokers' exposure to secondhand smoke—United States, 1999–2008. *MMWR Morb Mortal Wkly Rep* 59:1135–1140.
- Chen J, Bardes EE, Aronow BJ, Jegga AG. 2009. ToppGene suite for gene list enrichment analysis and candidate gene prioritization. *Nucleic Acids Res* 37:W305–W311.
- Colman GJ, Joyce T. 2003. Trends in smoking before, during, and after pregnancy in ten states. *Am J Prev Med* 24:29–35.
- Corradino R, De Palma C. 2011. PKG is the new regulator of Drp1 function. In: 35 Congresso Nazionale della Società Italiana di Farmacologia, September 14–17, Bologna, Italy. Bologna, Italy: Società Italiana di Farmacologia.
- Cortes DF, Landis MK, Ottens AK. 2012. High-capacity peptide-centric platform to decode the proteomic response to brain injury. *Electrophoresis*; doi:10.1002/elph.201200341.
- Dalwani M, Sakai JT, Mikulich-Gilbertson SK, Tanabe J, Raymond K, McWilliams SK, et al. 2011. Reduced cortical gray matter volume in male adolescents with substance and conduct problems. *Drug Alcohol Depend* 118:295–305.
- de Cerqueira Cesar M, Wilson JE. 2002. Functional characteristics of hexokinase bound to the type A and type B sites of bovine brain mitochondria. *Arch Biochem Biophys* 397:106–112.
- De Palma C, Falcone S, Pisoni S, Cipolat S, Panzeri C, Pambianco S, et al. 2010. Nitric oxide inhibition of Drp1-mediated mitochondrial fission is critical for myogenic differentiation. *Cell Death Differ* 17:1684–1696.
- Dobbing J. 1982. The later development of the brain and its vulnerability. In: *Scientific Foundations of Paediatrics* (Davis JA, Dobbing J, eds). Baltimore, MD: University Park Press, 744–759.
- Doherty SP, Grabowski J, Hoffman C, Ng SP, Zelkoff JT. 2009. Early life insult from cigarette smoke may be predictive of chronic diseases later in life. *Biomarkers* 14(suppl 1):97–101.
- Friede RL. 1973. Dating the development of human cerebellum. *Acta Neuropathol* 23:48–58.
- Fuller BF, Gold MS, Wang KK, Ottens AK. 2010. Effects of environmental tobacco smoke on adult rat brain biochemistry. *J Mol Neurosci* 41:165–171.
- Gosker HR, Hesselink MK, Duimel H, Ward KA, Schols AM. 2007. Reduced mitochondrial density in the vastus lateralis muscle of patients with COPD. *Eur Respir J* 30:73–79.
- Gospe SM Jr, Zhou SS, Pinkerton KE. 1996. Effects of environmental tobacco smoke exposure *in utero* and/or postnatally on brain development. *Pediatr Res* 39:494–498.
- Gramsbergen A. 1993. Consequences of cerebellar lesions at early and later ages: clinical relevance of animal experiments. *Early Hum Dev* 34:79–87.
- Hashimoto M, Wilson JE. 2000. Membrane potential-dependent conformational changes in mitochondrially bound hexokinase of brain. *Arch Biochem Biophys* 384:163–173.
- Kabir Z, Connolly GN, Alpert HR. 2011. Secondhand smoke exposure and neurobehavioral disorders among children in the United States. *Pediatrics* 128:263–270.
- Kanehisa M, Goto S, Furumichi M, Tanabe M, Hiraoka M. 2010. KEGG for representation and analysis of molecular networks involving diseases and drugs. *Nucleic Acids Res* 38:D355–D360.
- Kann O, Kovacs R. 2007. Mitochondria and neuronal activity. *Am J Physiol Cell Physiol* 292:C641–C657.
- Koop M, Rilling G, Herrmann A, Kretschmann HJ. 1986. Volumetric development of the fetal telencephalon, cerebral cortex, diencephalon, and rhombencephalon including the cerebellum in man. *Bibl Anat* 28:53–78.
- Li H, Chen Y, Jones AF, Sanger RH, Collis LP, Flannery R, et al. 2008. Bcl-x_i induces Drp1-dependent synapse formation in cultured hippocampal neurons. *Proc Natl Acad Sci USA* 105:2169–2174.
- Marano C, Schober SE, Brody DJ, Zhang C. 2009. Secondhand tobacco smoke exposure among children and adolescents: United States, 2003–2006. *Pediatrics* 124:1299–1305.
- McCormack MC, Breyse PN, Hansel NN, Matsui EC, Tonorez ES, Curtin-Brosnan J, et al. 2008. Common household activities are associated with elevated particulate matter concentrations in bedrooms of inner-city Baltimore pre-school children. *Environ Res* 106:148–155.
- Mouton PR. 2002. *Principles and Practices of Unbiased Stereology: An Introduction for Bioscientists*. Baltimore, MD: Johns Hopkins University Press.
- Oberg M, Jaakkola MS, Woodward A, Peruga A, Pruss-Ustun A. 2011. Worldwide burden of disease from exposure to second-hand smoke: a retrospective analysis of data from 192 countries. *Lancet* 377:139–146.
- O'Halloran CJ, Kinsella GJ, Storey E. 2012. The cerebellum and neuropsychological functioning: a critical review. *J Clin Exp Neuropsychol* 34:35–56.
- Ott W, Klepeis N, Switzer P. 2008. Air change rates of motor vehicles and in-vehicle pollutant concentrations from second-hand smoke. *J Expo Sci Environ Epidemiol* 18:312–325.
- Pastorino JG, Hoek JB. 2008. Regulation of hexokinase binding to VDAC. *J Bioenerg Biomembr* 40:171–182.
- Pauly JR, Slotkin TA. 2008. Maternal tobacco smoking, nicotine replacement and neurobehavioural development. *Acta Paediatr* 97:1331–1337.
- Richter S, Dimitrova A, Hein-Kropp C, Wilhelm H, Gizewski E, Timmann D. 2005. Cerebellar agenesis II: motor and language functions. *Neurocase* 11:103–113.
- Siskova Z, Mahad DJ, Pudney C, Campbell G, Cadogan M, Asuni A, et al. 2010. Morphological and functional abnormalities in mitochondria associated with synaptic degeneration in prion disease. *Am J Pathol* 177:1411–1421.
- Slotkin TA, Pinkerton KE, Garofolo MC, Auman JT, McCook EC, Seidler FJ. 2001. Perinatal exposure to environmental tobacco smoke induces adenylyl cyclase and alters receptor-mediated cell signaling in brain and heart of neonatal rats. *Brain Res* 898:73–81.
- Steinlin M. 2008. Cerebellar disorders in childhood: cognitive problems. *Cerebellum* 7:607–610.
- Stohr T, Schulte Wermeling D, Weiner I, Feldon J. 1998. Rat strain differences in open-field behavior and the locomotor stimulating and rewarding effects of amphetamine. *Pharmacol Biochem Behav* 59:813–818.
- Szklarczyk D, Franceschini A, Kuhn M, Simonovic M, Roth A, Minguez P, et al. 2011. The STRING database in 2011: functional interaction networks of proteins, globally integrated and scored. *Nucleic Acids Res* 39:D561–D568.
- Tiemeier H, Lenroot RK, Greenstein DK, Tran L, Pierson R, Giedd JN. 2010. Cerebellum development during childhood and adolescence: a longitudinal morphometric MRI study. *Neuroimage* 49:63–70.
- Uo T, Dworzak J, Kinoshita C, Inman DM, Kinoshita Y, Horner PJ, et al. 2009. Drp1 levels constitutively regulate mitochondrial dynamics and cell survival in cortical neurons. *Exp Neurol* 218:274–285.
- U.S. Department of Health and Human Services. 2006. *The Health Consequences of Involuntary Exposure to Tobacco Smoke: A Report of the Surgeon General*. O2NLM: WA 754 H4325 2006. Atlanta, GA: U.S. Surgeon General. Available: <http://www.surgeongeneral.gov/library/reports/secondhandsmoke/fullreport.pdf> [accessed 26 October 2012].
- U.S. Environmental Protection Agency. 1992. *Respiratory Health Effects on Passive Smoking: Lung Cancer and Other Disorders*. Publication 600/6–90/006F. Washington, DC: U.S. EPA. Available: http://oaspub.epa.gov/eims/eimscmm.getfile?p_download_id=36793 [accessed 26 October 2012].
- Valera EM, Faraone SV, Murray KE, Seidman LJ. 2007. Meta-analysis of structural imaging findings in attention-deficit/hyperactivity disorder. *Biol Psychiatry* 61:1361–1369.
- Westbrook DG, Anderson PG, Pinkerton KE, Ballinger SW. 2010. Perinatal tobacco smoke exposure increases vascular oxidative stress and mitochondrial damage in non-human primates. *Cardiovasc Toxicol* 10:216–226.
- Wu S, Zhou F, Zhang Z, Xing D. 2011. Mitochondrial oxidative stress causes mitochondrial fragmentation via differential modulation of mitochondrial fission-fusion proteins. *FEBS J* 278:941–954.